ISSN (Print) 1226-1750
ISSN (Online) 2233-6656
Journal of Magnetics 25(4), 469-474 (2020) https://doi.org/10.4283/JMAG.2020.25.4.469

Effect of Peritectic Banded Structure on Magnetic Properties of $SmCo_5$ Sintered Magnets

Saleem Akhtar[1], A. Nusair Khan[2]*, Mushtaq Khan[1], Syed Husain Imran Jaffery[1], and Arslan Saleem[3]

[1]School of Mechanical and Manufacturing Engineering (SMME), National University of Sciences and Technology (NUST), H-12, Islamabad, Pakistan
[2]Ibn-e-Sina Institute of Technology, H-11/4, Islamabad, Pakistan
[3]School of Mechanical Engineering & IEDT, Kyungpook National University, Daegu 41566, Republic of Korea

(Received 23 September 2019, Received in final form 10 November 2020, Accepted 11 November 2020)

$SmCo_5$ is well known for its high coercivity. However, still room is available to increase the coercive power of $SmCo_5$, since the theoretical values of the compound is far higher than the achieved values. Different attempts, in this regard, have been made either by controlling the microstructure or the chemical composition. However, it is noted that no or very few literature is available regarding the control of microstructure through solidification. Three types of $SmCo_5$ compound were prepared through induction melting technique so that final solidification be manipulated by controlling the mold temperature. Fractrographic analysis revealed a unique peritectic structure in $SmCo_5$ compound. It was observed that the peritectic plates, having nano-size thickness, remain present even after high temperature sintering operation. The nano-scale peritectic plates may affect the final magnetic properties, especially the coercivity of the subject compound.

Keywords : $SmCo_5$, Peritectic reaction, high coercivity

1. Introduction

The first part of this work is about the observation of banded structure obtained after peritectic reaction. It can be observed in Sm-Co phase diagram that for the chemical composition range where $SmCo_5$ exist, a peritectic reaction isotherm is present at 1300 ºC [1-4]. Further, it can be depicted from the phase diagram that this compound is not a stoichiometric compound. Different types of peritectic growth were reported by Hideyuki Yasuda *et al.* [5] for metallic alloys. In this regard, a banded structure growth is noted for lead-bismuth system. However, this type of growth was not reported before, in open literature, for $SmCo_5$ system, which is presented here.

The second part of this work is the reporting of ultra-high coercivity for $SmCo_5$, for sintered samples. Ultra high coercivity in $SmCo_5$ is the desire which was persuaded for the last many years. In this regard, chemical composition and microstructure control are the popular choice to manipulate the magnetic properties. Koppoju *et al.* [6] added 6.5 % copper in $SmCo_5$ and then melt spun the same at high velocity i.e. 50 m/s, achieving 52.7 kOe coercivity values, the measurements were made directly on the ribbons. Similarly, Fukuzaki *et al.* [7] made copper and iron additions and then melt spun the same obtaining 33 kOe coercivity. Fukuzaki *et al.* [7] also added tantalum along with iron and copper achieving 24.5 kOe intrinsic coercivity. The combination of iron and copper was also tried by Suresh *et al.* [8] and the achieved coercivity values were 32.7 kOe. Titanium addition is another option to enhance the coercivity of $SmCo_5$ and therefore, Yao *et al.* [9] tried and achieved upto 22.3 kOe coercivity. Huang *et al.* [10] added niobium, zirconium and copper in $SmCo_5$ and achieve the coercivity values upto 9 kOe. Addition of tin is made by Kundig *et al.* [11], Zaigham *et al.* [12] and Yao *et al.* [9] achieving coercivity 32 kOe, 1.0 kOe and 22.3 kOe respectively. Addition of chromium along with carbon was made by Li *et al.* [13], it was noted that the coercivity approached to 40.3 kOe. Similarly, nickel addition was made by Strzeszewski *et al.* [14] obtaining 16 kOe coercivity. Bian *et al.* [15] added AlNiCo alloy, a combination of Ni, Co, Al, Ti, Cu and Nb, in $SmCo_5$ achieving 19.6 kOe coercivity values.

Most of the microstructural control was made through

*Corresponding author: Tel: +923000539090
Fax: +92519034005, e-mail: engr_sakhtar@yahoo.com

strip or ribbon casting. For-example: Ding *et al.* [16] made ribbons of $SmCo_5$ and noted 30.5 kOe coercivity. Rong *et al.* [17] produced nano-powder achieving 26 kOe coercivity. Similarly, Yan *et al.* [18] melt spun the $SmCo_5$ and coercivity measured on the ribbons were 16.2 kOe. Chen *et al.* [19] produced the ribbons at 40 m/s achieving 16.2 kOe. However, strip and ribbon casting route is relatively expensive and need dedicated equipment. Further, Shen *et al.* [20] mentioned that sintering at high temperature lower the bulk coercivity by 2-3 times than that of the powder due to grain growth and structure and stress relaxation. It is worth to mention that the values of coercivity mentioned in the above cited work are mostly measured before sintering operation.

2. Experimental

Three induction melting has been done to produce $SmCo_5$ compound. For this purpose pure metals have been utilized. Addition of 5 % (by weight) extra samarium was made to compensate the samarium losses during the melting operation. During melting, the frequency (2.6 kHz) of induction coils also serves as a stirring agent and thus good homogeneity can be achieved. Pouring temperature for all the three castings was ensured to be the same by using the Fluke pyrometer. The molten pool was casted into an indigenously made water cooled copper plates mold. During casting the temperature of the cooling water, flowing through the mold, was controlled to achieve three relatively different types of castings. Therefore, the first casting was made at water inlet temperature of 4 ºC (from here on called "fast cooling"). The second casting was made at 18 ºC (from here on called "medium cooling") and the third casting was made at the inlet temperature of 30 ºC (from here on called "slow cooling"). Water mass flow rate i.e. 0.53 kg/s remain constant for all three castings.

The cooling rates for the three castings were calculated by using the Ansys-Fluid software. The properties taken for calculation are: density = 8300 kg/m^3, thermal conductivity = 12.78 W/m·K, specific heat = 334.9 J/kg·K.

After casting the ingots were crushed and ball milled to a final powder size: 3-6 micro-meters. During ball milling, the rotatory speed was kept at 150 rpm, while the ball to powder ratio was 6:1. No surfactant was used during the milling operation however, petroleum ether was utilized as a cooling agent. After 90 minutes ball milling, the final powder was first slightly pressed under 2 telsa magnetic field and then in cold iso-static chamber having 200 MPa pressure. The obtained brick like compacts were sintered at 1125 ºC in vacuum furnace for 80 minutes following the aging cycle at 900 ºC.

For material characterization the samples were taken both from as-cast and sintered samples. Fractrographic study was made on fresh fracture surfaces utilizing Scanning Electron Microscope (SEM). Further, the magnetic properties of all the sintered samples were observed on Pulse Field Magnetometer (PFM).

3. Results and Discussion

3.1. Finite element analysis for cooling rate

Three dimensional transient analysis has been performed on ANSYS-Fluent to investigate the cooling rate and solidification time of $SmCo_5$ in water cooled copper mold. The computational model consists of four domains i.e. copper plates that act as heat sink, molten $SmCo_5$, water that cools down the $SmCo_5$ metal and steel frame that encapsulates the whole setup. The computational cost has been reduced by modeling only half of the computational domain employing symmetry boundary condition. Whole computational domain has been discretized into structured hexahedral grid using ICEM-CFD.

Solidification model has been employed to simulate the phase change (solidification) of liquid $SmCo_5$ metal. Mass flow boundary condition has been enforced on the water inlet face and pressure outlet boundary condition has been used for water outlet face. Additionally, no-slip boundary condition has been utilized against all domain walls.

The time step size of 0.001 has been used to avoid divergence of the solution and the simulation has been run for 50,000 time steps. The computational results indicate that the cooling rate for 4×10^{-4} m^3 of liquid

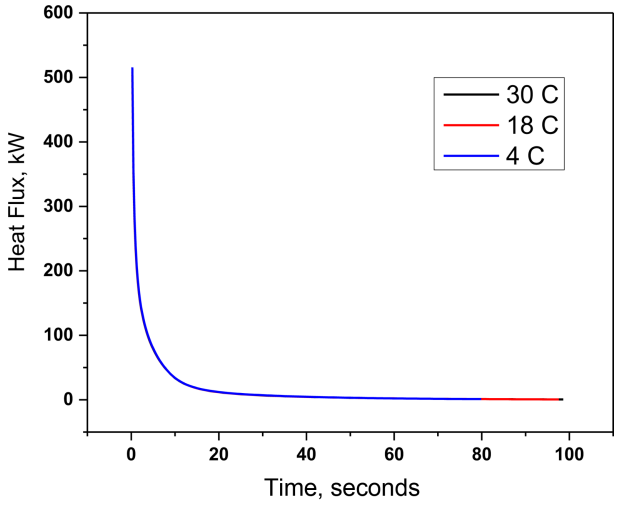

Fig. 1. (Color online) Dissipation of heat flux in water cooled copper mold with time.

metal is 90 K/s. No significant difference in cooling rate was observed whether the water inlet temperature of the mold was kept at 4 ºC or 30 ºC, Fig. 1.

3.2. Microscopic Evaluation

Fracture surface of the as-cast melts revealed brittle nature of fracture, mostly consists of cleavage surfaces. However, some regions preserve the original structure and demonstrated the banded structure. Figure 2-4, compare the formation of banded structure in three different as-cast samples. Colonies of the banded structure observed in the samples referred to the fact that these are not artifacts. The same was observed close and away from the surface of the casting. This shows that the cooling rate was enough to promote the banded structure in the whole thickness of the casting. The formation of the banded structure can be referred to the peritectic reaction. Thus when the temperature drops from 1300 ºC, the peritectic reaction occurred. Five types of peritectic solidification growth has been reported in the literature [5] including: 1) peritectic transformation, 2) peritectic reaction, 3) growth of phases in which secondary phase does not grow along the primary phase, 4) growth in banded structure, 5) growth in which fluctuated structure is obtained. In the banded structure the two constituent solid phases grow alternately. Energy Dispersive spectrometric (EDS) analysis revealed the variation of samarium contents in the range of 0.5 to 1.0 atomic percentage. This variation is noted on the crest and the adjacent trough of the banded structure.

During solidification process, the melt rejects the excessive samarium to the interface region. Therefore, ample time is required to assimilate the rejected samarium in the melt pool by diffusion method but by the virtue of high cooling rates the variations in samarium contents are arrested within the structure.

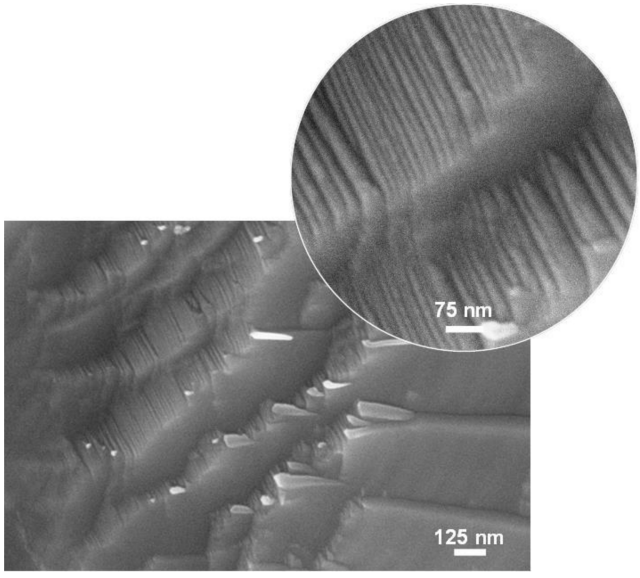

Fig. 2. Fracture surface revealing in as-cast sample. The peritectic banded structure revealed in fast cooled sample.

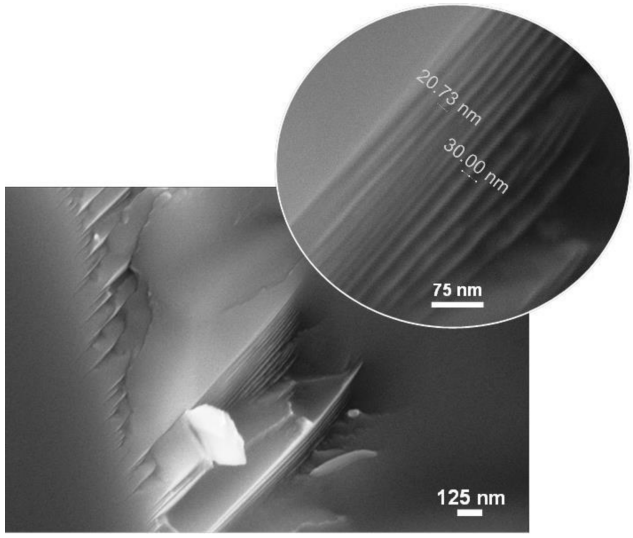

Fig. 3. Fracture surface revealing in as-cast sample. The peritectic banded structure revealed in medium cooled sample.

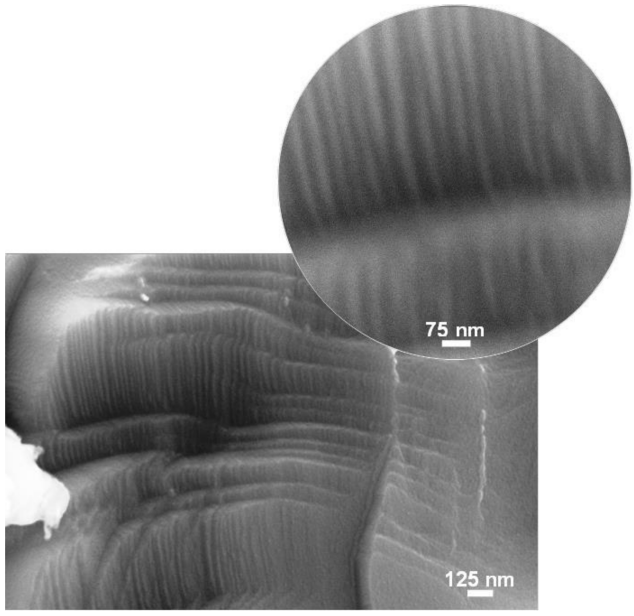

Fig. 4. Fracture surface revealing in as-cast sample. The peritectic banded structure revealed in slow cooled sample.

The banded structure obtained after solidification of $SmCo_5$ compound along with columnar grains. The direction of the columnar or cellular structure depends upon the heat extraction from the molten pool. In the subject mold the solidification of the melt is unidirectional which generates cells that grow in the opposite direction of the

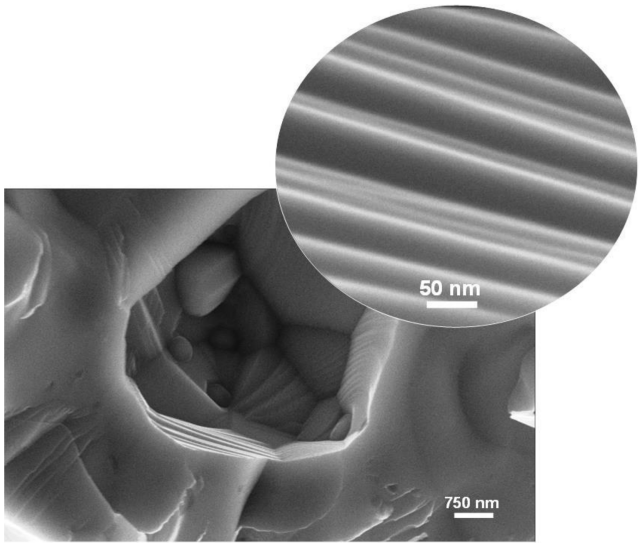

Fig. 5. Fracture surface revealing in sintered sample. The peritectic banded structure revealed in fast cooled sample.

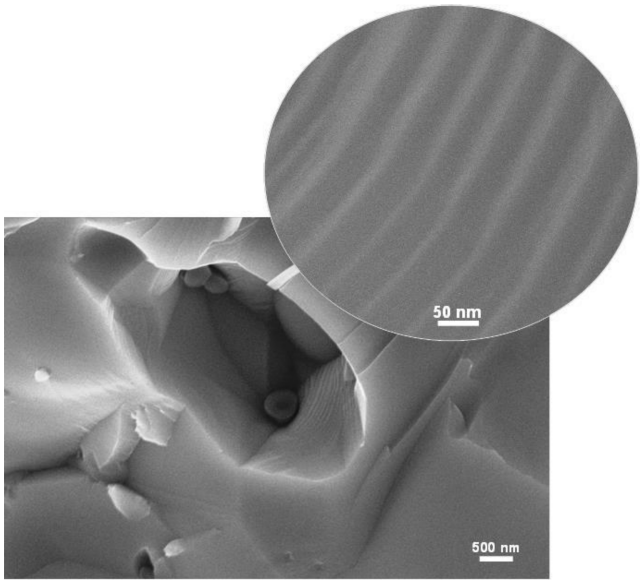

Fig. 6. Fracture surface revealing in sintered sample. The peritectic banded structure revealed in medium cooled sample.

heat flow in a non-crystallographic manner [21]. The size and shape obtained during or after the solidification process depends upon the nucleation and growth rate, for example, if the nucleation rate is high enough then the grain size will be fine. In directionally grown peritectics, as in our case where the heat dissipation is high, the microstructure pattern is determined by the dendrites or cells of the high-temperature phase. Thus the final microstructure can control the properties of the material [22].

After sintering the peritectic reaction product still exist in the samples but certainly grain growth was observed

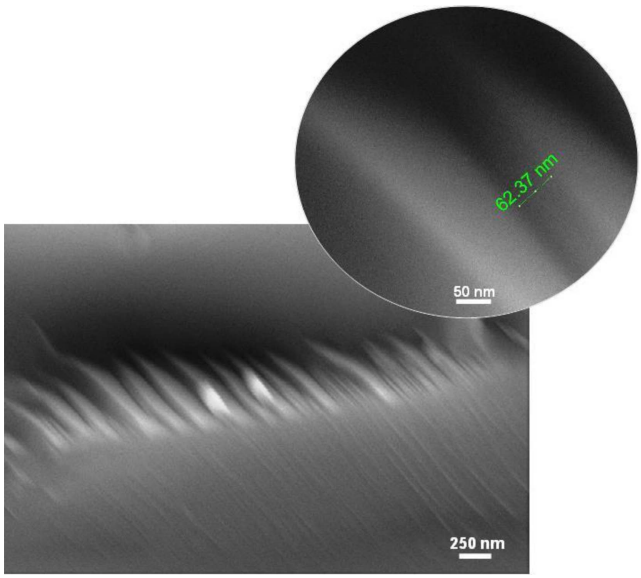

Fig. 7. Fracture surface revealing in sintered sample. The peritectic banded structure revealed in slow cooled sample.

Table 1. Diameter of peritectic banded structure observed in three conditions.

S.No.	Size, nm		
	Cooling Temp, ºC	As-cast, nm	Sintered sample, nm
1	Fast cooled	30-50	30-40
2	Medium cooled	20-130	28-55
3	Slow cooled	50-100	65-250

due to high temperature processing. Fracture surfaces observed after sintering demonstrated fine banded structure, Fig. 5-7. It was observed that the thickness of the peritectic banded structure remain same however, the frequency of observation was decreased. Table 1 demonstrates some data of the size of the banded structure i.e. thickness taken in as-cast condition and after sintering.

3.3. Magnetic Properties

The magnetic properties achieved for the three types of alloys are shown in M-H curves presented in Fig. 8. It can be seen that the samples having the finest peritectic structure demonstrated the highest coercivity values as compared to the other samples. When magnetic field applied to the magnetic sample, the moment of domain walls started and continuous to move till the saturation of the magnetization achieved. At saturation point, ideally, there is only one domain in the sample. Thus the domains annihilated during the magnetization. The pinning of the domain walls movement during the applied magnetic

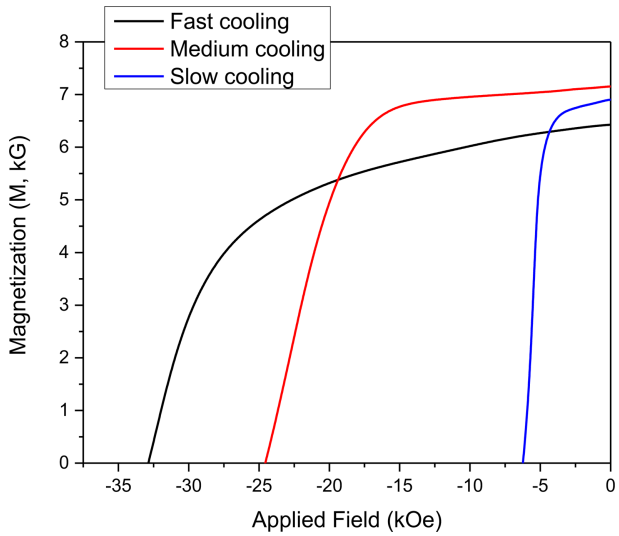

Fig. 8. (Color online) Second quadrant of the MH curve showing the intrinsic coercivity of the three samples.

field (H) cause to increase the coercivity of the sample. Since $SmCo_5$ domain wall thickness is around 2.6 nm [23] i.e. few atoms thickness therefore, domain walls will not expect to strongly interact with point defects like interstitial atoms observed at the boundaries of peritectic rods.

Grain boundaries are also act like domain boundary if for example; the adjacent grains have different orientations. These domain boundaries are though not similar to the regular domain boundaries because these do not move or reorient. In general, the increasing grain size allows the domain walls to move extensively than in smaller grains. Thus the increase in coercivity is attributed to the pinning of domain walls at the boundaries of the peritectic rods. These grain boundaries or peritectic rod boundaries hinder the growth of domain walls from grain to grain [24].

The remanance ratio i.e. Mr/Ms [25] for all the three types of sample is good. The high cooling sample demonstrated 0.923, medium cooled sample showed 0.973 while the low cooled sample having 0.996 value. Similarly, the squareness of the curve which is defined by the ratio Hk/Hc [10] is 0.95 for all the three samples. The magnetization stability (Hk/4πMr) [6] is revealed maximum for high cooling sample i.e. 0.386 and for medium and low cooled sample it was 0.259 and 0.068 respectively.

4. Conclusion

Three inlet water temperatures are used to control the microstructure of the final cast product. It is noted through Ansys calculations that no significant difference is in the cooling rate of the three melts. Fractographic study revealed peritectic banded structure which apparently affect the coercivity of the sintered $SmCo_5$ magnets. High coercivity along with relatively better magnetic stability was noted for the samples having relatively finer peritectic banded structure.

References

[1] L. Cataldo, A. Lefevre, F. Ducret, M.-Th. Cohen-Adad, C. Allibert, and N. Valignat, J. Alloys Compd. **241**, 216 (1996).
[2] S. Aich and J. E. Shield, J. Magn. Magn. Mater. **279**, 76 (2004).
[3] J. F. Miller and A. E. Austin, J. Cryst. Growth **18**, 7 (1973).
[4] J. F. Miller and A. E. Austin, Journal of Less Common Metals **25**, 317 (1971).
[5] Solidification and Casting Series in Materials Science and Engineering, Eds. Brain Cantor, Keyna O'Reilly, Institute of Physics Publishing, Bristol and Philadelphia, (2003) Hideyuki Yasuda, Itsuo Ohnaka, Kentaro Tokieda, Naohiro Notake, Peritectic solidification, chapter 11, p 160.
[6] S. Koppoju, V. Chandrasekaran, and R. Gopalan, AIP Advances **5**, 077118 (2015).
[7] T. Fukuzaki, H. Iwane, K. Abe, T. Doi, R. Tamura, and T. Oikawa, J. Appl. Phys. **115**, 17A760 (2014).
[8] K. Suresh, R. Gopalan, G. Bhikshamaiah, A. K. Singh, D. V. Sridhara Rao, K. Muraleedharan, and V. Chandrasekaran, J. Alloys Compd. **463**, 73 (2008).
[9] Zan Yao, Qi Xu, Chengbao Jiang Zan Yao, Qi Xu, and Chengbao Jiang, J. Magn. Magn. Mater. **320**, 1717 (2008).
[10] M. Q. Huang, Z. Turgut, B. M. Ma, Z. M. Chen, D. Lee, A. Higgins, C. H. Chen, S. Liu, S. Y. Chu, J. C. Horwath, and R. T. Fingers, J. Appl. Phys. **103**, 07E134 (2008).
[11] A. A. Kundig, R. Gopalan, T. Ohkubo, and K. Hono, Scripta Materialia **54**, 2047 (2006).
[12] H. Zaigham and F. A. Khalid, Mater. Charact. **61**, 1274 (2010).
[13] Liya Li, Zhi Gao, Yicheng Ge, Aru Yan, Wei Zhang, and Yuandong Peng, J. Alloys Compd. **714**, 194 (2017).
[14] J. Strzeszewski and G. C. Hadjipanayis, J. Appl. Phys. **67**, 4595 (1990).
[15] Lu-peng Bian, Ying Li, Xu-hao Han, Jin-yun Cheng, Xiao-ning Qin, Yan-qiu Zhao, and Ji-bing Sun, Physica B: Condens. Matter. **531**, 1 (2018).
[16] J. Ding, P. G. McCormick, and R. Street, J. Alloys Compd. **228**, 102 (1995).
[17] C. Rong N. Poudyal, X. B. Liu, Y. Zhang, M. J. Kramer, and J. Ping Liu, Appl. Phys. Lett. **101**, 152401 (2012).
[18] A-ru Yan, Wen-yong Zhang, Hong-wei Zhang, and Bao-gen Shen, J. Magn. Magn. Mater. **210**, L10 (2000).
[19] S. K. Chen, M. S. Chu, and J. L. Tsai, IEEE Trans. Magn. **32**, 4419 (1996).

[20] Y. Shen, S. Leontsev, A. O. Sheets, J. C. Horwath, and Z. AIP Advances **6**, 056005 (2016).
[21] Direct strip casting of metals and alloys Processing, microstructure and properties, Michael Ferry, Woodhead Publishing and Maney Publishing, The Institute of Materials, Minerals & Mining (2006) CRC Press, Boca Raton, FL 33487, USA.
[22] Solidification and Casting; Series in Materials Science and Engineering Eds. Brain Cantor, Keyna O'Reilly, Institute of Physics Publishing, Bristol and Philadelphia, (2003) John Hunt, Pattern formation during solidification, chapter 10, p 143.
[23] Magnetism and Magnetic Materials J.M.D. Coey, Cambridge university press, UK (2009).
[24] Permanent Magnets and Electo-mechanical devices Ed. Edward P. Furlani, Acadamic Press (2001) p 51.
[25] W. Y. Zhang X. D. Zhang, Y. C. Yang, and B. G. Shen, J. Alloys Compd. **353**, 274 (2003).